Atmos. Chem. Phys. Discuss., 13, 6807–6849, 2013
www.atmos-chem-phys-discuss.net/13/6807/2013/
doi:10.5194/acpd-13-6807-2013

Atmospheric Chemistry and Physics Discussions

Atmospheric nitric oxide and ozone at the WAIS Divide deep coring site: a discussion of local sources and transport in West Antarctica

S. Masclin[1], M. M. Frey[2,1], W. F. Rogge[1,3], and R. C. Bales[1,3]

[1]Environmental Systems, University of California, Merced, California, USA
[2]British Antarctic Survey, Natural Environment Research Council, Cambridge, UK
[3]Sierra Nevada Research Institute, University of California, Merced, California, USA

Received: 18 December 2012 – Accepted: 26 February 2013 – Published: 14 March 2013

Correspondence to: S. Masclin (smasclin@ucmerced.edu)

Published by Copernicus Publications on behalf of the European Geosciences Union.

Abstract

First measurements of atmospheric nitric oxide (NO) along with observations of ozone (O_3), hydroperoxides (H_2O_2 and MHP) and snow nitrate (NO_3^-), on the West Antarctic Ice Sheet (WAIS) were carried out at the WAIS Divide deep ice-coring site between 10 December 2008 and 11 January 2009. Average $\pm 1\sigma$ mixing ratios of NO were 19 ± 31 pptv and confirmed prior model estimates for the summer boundary layer above WAIS. Mean $\pm 1\sigma$ mixing ratios of O_3 of 14 ± 4 ppbv were in the range of previous measurements from overland traverses across WAIS during summer, while average $\pm 1\sigma$ concentrations of H_2O_2 and MHP revealed slightly higher levels with mixing ratios of 743 ± 362 and 519 ± 238 pptv, respectively.

An upper limit for daily average NO_2 emission fluxes of $4.6–6.6 \times 10^8$ molecule cm^{-2} s^{-1} was estimated based on photolysis of measured NO_3^- in surface snowpack. Assuming rapid and complete mixing into the overlying atmosphere, and steady state of NO_x, these snow emissions are equivalent to an average (range) production of atmospheric NO_2 of 7 (2–53) pptv h^{-1} for a typical atmospheric boundary-layer depth of 130 (490–20) m.

This indicates that local emissions from the snowpack are a significant source of short-lived nitrogen oxides above the inner WAIS.

The origins of the air masses reaching WAIS Divide during this campaign were investigated with a 4-day back-trajectory analysis every 4 h. The resulting 168 back trajectories revealed that in 73 % of all runs air originated from East Antarctic Plateau regions below 2500 m (41 %), coastal Antarctica (17 %) and inner WAIS (15 %). For these air sources O_3 levels were on average 13 ± 3 ppbv. The remaining 27 % are katabatic outflows from the East Antarctic Plateau above 2500 m. When near-surface air from the East Antarctic Plateau reaches WAIS Divide through a rapid transport of less than 3 days, O_3 levels are on average 19 ± 4 ppbv with maximum mixing ratios of 30 ppbv. Episodes of elevated ozone at WAIS Divide are therefore linked to air mass export off the East Antarctic Plateau, demonstrating that outflows from the highly oxidizing sum-

ACPD
13, 6807–6849, 2013

mer atmospheric boundary layer in the interior of the continent can episodically raise the mixing ratios of long-lived atmospheric chemical species such as O_3 and enhance the oxidative capacity of the atmosphere above WAIS.

1 Introduction

Over the last decade, a large number of field and lab studies have provided evidence of the importance of snow photochemistry on the chemical composition of air above snow-covered surfaces in the polar and mid latitudes (Abbatt et al., 2012; Grannas et al., 2007, and references therein). The upper snowpack is seen not only as a chemical reservoir but as a chemical reactor. Trace gases emitted by the snowpack include hydrogen peroxide (H_2O_2), formaldehyde (CH_2O) and nitrogen oxides ($NO_x = NO + NO_2$), and increase the oxidizing potential of the atmospheric boundary layer through production of the hydroxyl radical (OH) and ozone (O_3) (Thomas et al., 2012; Grannas et al., 2007, and references therein).

Measurements of atmospheric and snow concentrations and also fluxes from snow surfaces indicate that the polar snowpack emits NO_x mainly through the photolysis of nitrate (NO_3^-) in near-surface snow (Frey et al., 2012; Bauguitte et al., 2012; Frey et al., 2009b; Grannas et al., 2007; Jones et al., 2000; Honrath et al., 1999). Snowpack emissions of NO_x can contribute significantly to the NO_y (NO_x + other oxidized nitrogen species) budget above snow, as observed in continental and coastal Antarctica (Frey et al., 2012; Jones et al., 2000). Bauguitte et al. (2012) reached a similar conclusion at Halley station by highlighting that halogen chemistry over the Antarctic coast controls the lifetime of NO_x species and reduces the nitric oxide (NO) mixing ratios. When atmospheric turbulence is low or atmospheric boundary layer (ABL) depths shallow, these emissions contribute to high NO_x levels, several 100 s pptv, as observed at South Pole and over the East Antarctic Plateau (Frey et al., 2012; Slusher et al., 2010; Davis et al.,

ACPD
13, 6807–6849, 2013

2008, 2004). Chen et al. (2004) and Mauldin et al. (2004) showed that at South Pole these high levels of NO_x shift the HO_x ($OH + HO_2$) partitioning towards OH:

$$NO + HO_2 \rightarrow NO_2 + OH \quad \text{(R1)}$$

NO_x emissions from snow can also lead to net production of O_3 over the East Antarctic Plateau (Helmig et al., 2008a,b; Crawford et al., 2001), and thereby shift HO_x partitioning of the overlying atmosphere.

Above the West Antarctic Ice Sheet (WAIS) enhanced snowpack emissions of NO_x associated with events of stratospheric ozone depletion may lower the formation rate of atmospheric H_2O_2 (Frey et al., 2005). Photochemical modeling suggests that atmospheric H_2O_2 is sensitive to the NO background, opening up the possibility to constrain past NO_x and OH levels using the H_2O_2 ice core record (Frey et al., 2006, 2005). Therefore, investigation of the current atmospheric boundary layer photochemistry at a WAIS ice-core drilling site is essential to interpret ice-core records of photochemically active species such as H_2O_2 and NO_3^-. This can also provide essential information regarding the contribution of air advection from the East Antarctic Plateau to the levels of oxidants above WAIS, as Legrand et al. (2009) showed that air outflows from the Antarctic Plateau raise the O_3 levels of the East Antarctic coastal site Dumont D'Urville.

So far, atmospheric sampling campaigns in the Antarctic have taken place at existing stations on the coast (Dumont D'Urville, Halley, Neumayer) and on the East Antarctic Plateau (South Pole, Dome C). Only recent airborne campaigns (Slusher et al., 2010; Eisele and Davis, 2008) or scientific over-land traverses (Frey et al., 2005) provided information on the composition of the lower atmosphere across the interior of the continent. Thus spatial data coverage of the lower atmosphere in Antarctica is still sparse and little is known about the variability of ozone and its precursors above WAIS. For example, the first ground based measurements across WAIS lasting several days included atmospheric records of H_2O_2, methyl hydroperoxide (MHP), CH_2O, O_3 but not NO_x (Frey et al., 2005).

The study included multi-week first observations of NO and complementary measurements of atmospheric O_3, H_2O_2, MHP and of surface-snow H_2O_2, NO_3^- and nitrite

ACPD
13, 6807–6849, 2013

(NO_2^-) in the WAIS region. The aims were to determine the summer composition of the lower atmosphere in the interior of West Antarctica and the relative importance of local production versus air-mass transport on the local atmospheric budgets of NO_x and O_3.

2 Methods

From 10 December 2008 to 11 January 2009, atmospheric concentrations of NO and O_3 were continuously measured at WAIS Divide (local solar time: LST = UTC – 7:30). Mixing ratios of ROOH (H_2O_2 and MHP) were recorded between 31 December 2008 to 7 January 2009. Snow samples were collected daily from the surface and weekly from 30-cm snow pits for chemical analysis of NO_3^-, NO_2^- and H_2O_2.

Atmospheric sampling took place 5 km NW of the WAIS Divide drilling camp (79.467° S, 112.085° W, 1766 m a.m.s.l., http://www.waisdivide.unh.edu). All instruments were run out of a Polarhaven tent heated by a preway heater. Atmospheric measurements were made 1 m above the snow, 10-m upwind (prevailing winds from NE) from the tent, with ambient air drawn through an insulated and heated PFA (1/4″ I.D.) intake line (typically 1.4 STP – L min^{-1}) for ROOH, O_3, and NO. In an attempt to minimize artifacts in our atmospheric records, the two generators (3.5 and 5 KW) that provided electricity to the lab were located about 30 m downwind from the sampling lines, and all activities around the site were restricted. However, the heater exhaust was located on the top of the Polarhaven tent.

2.1 Atmospheric sampling

NO was measured using a modified chemiluminescence instrument used previously at South Pole (Davis et al., 2004, 2001). NO mixing ratios recorded at 1 Hz were aggregated to 1-min averages. The limit of detection (LOD), defined as 2-σ of the background count rate, was 5 pptv. A two-minute background signal was monitored every 20 min and an automatic 4-min calibration was performed every 2 h by addition of

ACPD
13, 6807–6849, 2013

a 2 ppmv NO standard. Due to late delivery of this NO gas standard to the site, calibration was only run during the last 3 days of the campaign. The instrument sensitivity remained fairly constant over the three days, with an average over 16 calibrations of $7.10 \pm 0.18\,\mathrm{Hz\,pptv^{-1}}$, similar to the pre-season value of $7.00\,\mathrm{Hz\,pptv^{-1}}$ determined in the lab. We therefore used the 3-day average value of these calibrations to process the overall dataset. NO spikes related to pollution from generators and heater exhaust were removed using a moving standard deviation filter with a maximum standard deviation of 30 (1.5 times the inter-quartile range of the dataset). This led to the removal of 25 % from the raw NO record.

Surface O_3 was monitored at 1-min resolution using a 2B Technologies (Golden, Colorado) ozone monitor, model 205, similar to those previously used in the remote Antarctic such as on the ITASE traverses (Frey et al., 2005) and in a ozone monitor network (Bauguitte et al., 2011). LOD was 1 ppbv.

Atmospheric ROOH were measured based on continuous scrubbing of sample air followed by separation in an HPLC column and fluorescence detection described in detail by Frey et al. (2005, 2009a). The detector was calibrated 1–2 times per day with H_2O_2 solution and MHP standards synthesized in our lab following the protocol described by Frey et al. (2009a). The LOD, 2-σ of the baseline, were 87 pptv for H_2O_2 and 167 pptv for MHP. Unexpected variations of the coil-scrubber temperatures may have caused higher LOD than those reported by Frey et al. (2005, 2009a).

2.2 Snow sampling

All surface snow and snow pits were sampled in a 7200-m^2 clean area upwind from the Polarhaven tent. The top 1 cm of snow was collected daily with a 10-ml glass test tube to assess temporal changes in snow chemistry. Twice during the campaign, surface snow was sampled simultaneously at five different spots inside the clean area to assess possible local spatial variability of NO_3^-, NO_2^- and H_2O_2.

Weekly snow pits were sampled at 2-cm resolution to a depth of 30 cm, covering the snowpack zone where 85 % of the nitrate photolysis is expected to occur (France et al.,

ACPD
13, 6807–6849, 2013

2011). Snowflakes were collected on aluminum foil during the only snow precipitation event observed during the campaign, on 12 December 2008.

All snow samples were collected in 100-ml SCHOTT bottles and kept frozen during storage and transport until analysis 14 months later. The analysis involved melting the snow 1 h before injecting the sample into a self-built continuous flow analysis (CFA) system, as described by Frey et al. (2006). The LOD, defined as 3σ of the baseline, was 0.4 ppbw for NO_3^-, NO_2^- and H_2O_2. Only values above LOD were used for further calculations. Some loss of NO_2^- in the samples may have occurred between the time of collection and analysis, as O'Driscoll et al. (2012) and Takenaka and Bandow (2007) showed that nitrite may be oxidized during freezing and storage.

3 Results

3.1 Atmospheric concentrations

Some noise remained in the NO dataset filtering, but comparison to the 4-h running median (Fig. 1a) shows very little change in the overall trend of the data, with the median value after filtering similar to the one of the raw dataset. The average $\pm 1\sigma$ (median) of NO over the campaign were 19±31 (10) pptv (Table 1). One-minute data did not exhibit any clear diel cycle (Fig. 1), but 1-h bin centered data on each hour revealed a diel cycle that can be interpreted with the variations of the average solar elevation angle (Fig. 2). NO mixing ratios increased at 07:00–08:00 LST with a maximum rise of 36 % from the daily median. A decrease was observed afterwards and followed by a second increase of 20 % above the median value at 19:00 LST. These peaks in NO occurred as solar elevation angle increased and decreased with lower values of NO at the maxima and minima of solar elevation angle.

Average $\pm 1\sigma$ (median) mixing ratios of surface ozone at WAIS Divide were 14 ± 4 (13) ppbv (Table 1). The mean is two thirds of the 20 ± 2 average mixing ratio observed at Byrd Station in summer 2002, but is in the range of values from previous measure-

ACPD
13, 6807–6849, 2013

ments between 79.06° S and 85.00° S above the WAIS (Frey et al., 2005) (Fig. 3). Two events of elevated O_3 levels were recorded between 24 and 25, and between 27 and 29 December with concentrations in the range of 20 to 30 ppbv (Fig. 1). Concentrations above 25 ppbv were only observed for winds blowing from ENE to SWS. This wind sector represents 67 % of all the wind directions observed during the field campaign (Fig. 4).

Concentrations of H_2O_2 and MHP were measured between 31 December 2008 and 5 January 2009 (Fig. 1). Averages $\pm 1\sigma$ (medians) were 743 ± 362 (695) and 519 ± 238 (464) pptv for H_2O_2 and MHP, respectively. Our records are closer to values observed at lower altitude and slightly higher than measurements made in the surrounding area (Fig. 3), with mixing ratios of H_2O_2 that were twice those observed at Byrd station in late November 2002 (Table 1). Average $\pm 1\sigma$ (range) of the MHP : (H_2O_2+MHP) ratios were 0.42 ± 0.10 (0.12–0.76). These values are in the range of those previously recorded over WAIS (Frey et al., 2005). Daily binned values suggest both H_2O_2 and MHP presented a diel cycle with a respective maximum 44 and 37 % increase from their medians (695 and 464 pptv, respectively) observed in the morning (Fig. 2).

3.2 Concentrations in snow

Average $\pm 1\sigma$ (median) concentrations of NO_2^-, NO_3^- and H_2O_2 in surface snow at WAIS Divide were 0.6 ± 0.4 (0.5), 137 ± 37 (141) and 238 ± 37 (238) ppbw respectively (Table 1). Daily concentrations of NO_2^- in surface snow exhibited a decrease of 30 pptw per day ($R^2 = 0.36$) over the campaign (Fig. 5). This decrease represents a rate of 5 % per day of the average concentration of nitrite measured in all the snow-surface samples. Unlike NO_2^-, NO_3^- and H_2O_2 exhibited some variation but no trend was observed for these species.

Calculating the ratio of the standard deviation of the daily surface-snow concentrations to the mean of these concentrations allowed us to estimate the coefficient of variation of NO_2^-, NO_3^- and H_2O_2. Values of 49 %, 26 % and 17 % were found for NO_2^-,

ACPD
13, 6807–6849, 2013

NO_3^- and H_2O_2, respectively. Coefficients of variation for the simultaneous samplings made on 1 and 8 January 2009 (Fig. 5) are 17 %, 31 % and 7 % for NO_2^-, NO_3^- and H_2O_2, respectively. The close values of the NO_3^- coefficients suggest that variation of surface-snow NO_3^- may reflect both spatial and temporal variability. For NO_2^- and H_2O_2, the coefficients of temporal variability (49 % and 17 %, respectively) are more than double those calculated from spatial variability (17 % and 7 %, respectively). The variations of daily concentrations of NO_2^- and H_2O_2 in near-surface snow may then be interpreted as temporal trends. The variability between each sampling of H_2O_2 concentrations in the top 5 cm of the profile (Fig. 6) may also indicate a temporal trend: the high concentrations measured at the surface on 18 December were also measured at 4-cm depth on 28 December and at 6-cm depth on 4 January. This layer was apparently buried in snow from the first to the last day of snow-pit sampling.

The 30-cm deep profiles of NO_2^-, NO_3^- and H_2O_2, illustrated in Fig. 6, represent concentration changes of these species in snow over the last 6 months of 2008, based on local mean annual snow accumulation rate of 0.20 $m_{weq}\,yr^{-1}$ (Banta et al., 2008) and a measured snow density of 0.37. Total concentrations of NO_3^- in the snow column dropped from 720.4 to 581.0 ppbw between the first and last snow-pit samplings. Drops of NO_3^- between 94–188 ppbw were observed in the top 10 cm of each snow pit, whereas concentrations of ~ 30 ppbw were measured below. Total NO_2^- concentrations in the 30-cm column decreased slightly from 16.7 to 6.0 ppbw across the three snow-pit samplings. Unlike NO_2^- and NO_3^-, total concentrations of H_2O_2 in the top 30 cm of snowpack increased over the 18 days of sampling, from 940.6 ppbw to 2806.9 ppbw. A 233–298 ppbw decrease of H_2O_2 concentrations in the first 10 cm of each snow pit was generally observed.

ACPD
13, 6807–6849, 2013

4 Discussion

4.1 Local photochemistry

4.1.1 Factors controlling atmospheric levels of ROOH, NO, O_3 and snow content of NO_3^-, NO_2^- and H_2O_2

Levels of NO and O_3 measured at WAIS Divide during summer 2008–2009 are slightly higher than coastal values but lower than observed concentration on the Antarctic Plateau (Fig. 3). The observed mean of NO mixing rates are close to the 10 pptv predicted by Frey et al. (2005) at Byrd, about 160 km from WAIS Divide, using NASA Goddard Flight Center (GSFC) point photochemical model runs that included physical sources of H_2O_2 and CH_2O. H_2O_2 concentrations at WAIS Divide are similar to those observed above WAIS at lower latitudes (below 1500 m elevation) but 3 times the mixing ratios measured at South Pole (Frey et al., 2009a). As shown in Table 1 and in Fig. 3, the concentrations of H_2O_2 measured at WAIS Divide are higher than those measured at nearby sites (Frey et al., 2005). NO_3^- values are closer to values measured at coastal sites such as Halley or Neumayer stations (Mulvaney et al., 1998), than to the values observed at higher-altitude sites such as South Pole and Concordia stations (France et al., 2011; Traversi et al., 2009; Dibb et al., 2004; Rothlisberger et al., 2000). Being from a geographically intermediate site between the Antarctic coast and the East Antarctic Plateau, our results show that the atmospheric concentrations of NO, O_3, H_2O_2 above the WAIS during summer 2008–2009 are similar to coastal atmospheric levels. This indicates the possibility of using concentrations of radicals such as OH and HO_2 measured at Antarctic coastal sites in the calculations of NO_2 production in snow developped in Sect. 4.1.4.

The daily cycle of NO at WAIS Divide (Fig. 2) looks similar to the one that was observed at Summit/Greenland (Thomas et al., 2011), but with lower mixing ratios and a daily amplitude of 6.5 pptv. The 36 % rise from the NO median of 10.4 pptv along the increase of solar elevation angle suggests that the increase of solar elevation angle

ACPD
13, 6807–6849, 2013

enhances the photolytic production of NO. The decrease observed after 09:00 LST at high solar elevation angle may result from the increase of the atmospheric boundary layer height that enhances the dilution of near-surface NO into the overlying troposphere. The maximum wind speeds observed at 13:00–14:00 LST may indicate an increase of turbulent mixing and therefore efficient vertical upward transport and dilution of emissions at the surface (Frey et al., 2012). However, no measurement of the diel variability of the atmospheric boundary layer depth were performed during the campaign to confirm this point. The increase of NO levels by 20 % of the median value between 17:00–21:00 LST may result from the decrease of the atmospheric boundary layer height and wind speed along with solar elevation angle. 2-h binned data of NO and wind speed suggest that higher NO mixing ratios were observed for wind speeds less than $3\,m\,s^{-1}$.

O_3 did not exhibit any diel cycle with solar elevation angle or wind speed, which is consistent with a chemical lifetime on the order of days (Helmig et al., 2007b; Albert et al., 2002). It also may indicate that local O_3 production is a not a significant source of surface O_3 at WAIS Divide as discussed further below (Sect. 4.1.5). The ENE to SWS wind directions associated with high O_3 values (Fig. 4) indicate a possible contribution of air-mass transport to O_3 at WAIS Divide, with a potential impact of outflow from the Antarctic Plateau (see Sect. 4.2).

H_2O_2 and MHP exhibited a simultaneous increase with solar elevation angle between 3:00–13:00 LST, followed by a decrease at noon (Fig. 2). The maximum amplitude is observed at at noon (Fig. 2). The maximum amplitude is observed at 05:00 LST, a rise of 43 % above the median value of 695 pptv for H_2O_2. For MHP, mixing ratios rose to a maximum of 37 % above the median (464 pptv) at 05:00 and 13:00 LST. These results also suggest that mixing ratios of both H_2O_2 and MHP may be affected by an increase of the atmospheric boundary layer depth during the day. Unlike NO, ROOH did not show an increase in the second part of the day but the levels remained low, consistent with an increased uptake by the snowpack when the temperature decreased in the evening (Frey et al., 2009a; Hutterli et al., 2001, 2004; Bales et al., 1995). The

ACPD
13, 6807–6849, 2013

temperature record at the WAIS Divide camp was, however, too intermittent to further investigate the influence of temperature on atmospheric H_2O_2. A source from the snowpack is not considered significant for MHP since it has a solubility only 0.1 % that of H_2O_2 (Lind and Kok, 1994) and because no MHP has been detected in snow and ice above the current LOD (Frey et al., 2005, 2009a). The change of MHP may depend on the photochemistry of its precursors such as CH_4, NMHCs and water vapor, which may decrease with solar elevation angle. Higher H_2O_2 and MHP levels at low wind speed (below 4 $m\,s^{-1}$) suggest that ROOH are produced locally, reinforcing the conclusion of Frey et al. (2009a). They are then diluted through turbulent transport after production.

NO_3^- concentrations in surface snow present short-term and local spatial variations as Jarvis et al. (2009) and Wolff et al. (2008) also observed at Summit and Halley. These variations can not be explained with a scenario of fresh snowfall since only one snow precipitation occurred during the campaign. Some of these variations can be attributed to some events of snow removed by the wind since this snow removal would also impact on other chemical species than NO_3^-, such as H_2O_2 that presents similar variations than NO_3^- on 26–27 December 2008 and on 1–2 January 2009. However, these events are too episodic to explain the overall variations of surface-snow NO_3^-. It is suggested that part of NO_3^- in the top snowpack undergoes some possible post-depositional processes such as photolysis.

Low concentrations of NO_3^- and H_2O_2 related to the snowfall samples (Fig. 5) suggest that either the snow may have degassed during its collection, or prior to analysis. Anastasio and Robles (2007) showed that NO_3^- and H_2O_2 contribute to half the light absorption in polar snow for wavelengths of 280 nm and above. Since the snowflakes from this diamond-dust-like precipitation stayed exposed to the sun under a clear sky until their collection at the end of the event – over 5 h – it is possible that photochemical loss of NO_3^- and H_2O_2 may have occurred during the collection process.

The NO_3^- and H_2O_2 profiles measured in the 30-cm snow pits show both a summer peak as observed in earlier studies (Kreutz et al., 1999, and references therein). The increase over the campaign of H_2O_2 concentrations in the top 5 cm of snow (Fig. 6) may

ACPD
13, 6807–6849, 2013

point to a significant deposition of H_2O_2 during summer. NO_3^- in surface snow does not show a constant increase with time unlike H_2O_2. However, an 80 % decrease of NO_3^- concentrations with increasing depth in the snow is observed, similar to measurements from Dome C (France et al., 2011). Based on the interpretation of these authors, this decrease may therefore indicate that NO_3^- in the top snowpack can be significantly reduced by photolysis. A similar photochemical depletion can be suggested to explain the slight decrease of NO_2^- concentration observed in the 30-cm deep profiles over the campaign.

4.1.2 Steady-state estimation of atmospheric NO_2

Considering the NO-NO_2-O_3 system, it is reasonable to assume a photo-stationary steady state between NO and NO_2 at 1 m above the snowpack (Frey et al., 2012) to infer the potential atmospheric NO_2 concentrations from reactions:

$$NO_2 + h\nu \rightarrow NO + O(^3P) \quad \text{(R2)}$$

$$O(^3P) + O_2 + M \rightarrow O_3 + M \quad \text{(R3)}$$

$$NO + O_3 \rightarrow NO_2 + O_2 \quad \text{(R4)}$$

The conversion of NO to NO_2 described in Reaction (R4) is also achieved through different channels (Reactions R1, R5–R6) with the presence of oxidants such as HO_x, peroxy (RO_2) or halogen (XO=ClO, BrO) radicals:

$$NO + RO_2 \rightarrow NO_2 + RO \quad \text{(R5)}$$

$$NO + XO \rightarrow NO_2 + X \quad \text{(R6)}$$

NO_2 mixing ratios can therefore be estimated from the extended Leighton ratio as derived in (Ridley et al., 2000):

$$[NO_2] = [NO]\frac{k_{R4}[O_3] + k_{R1}[OX]}{j_2} \quad (1)$$

ACPD
13, 6807–6849, 2013

where the total radical concentration $[OX] = [HO_2] + [RO_2] + 2[XO]$ (Ridley et al., 2000). The photolytic rate constant j_2 was calculated from the NCAR/ACD radiative transfer model TUV version 5.0 (Lee-Taylor and Madronich, 2002) with O_3 columns measured by Total Ozone Mapping Spectrometer TOMS (http://ozoneaq.gsfc.nasa.gov/ozone_overhead_all_v8.md) and assuming clear-sky conditions. k_{R4} and k_{R1} were estimated through the temperature-dependent expressions from Sander et al. (2006). Halogen radicals were not considered into these calculations since no records have yet been reported above WAIS. Using the averages of NO and O_3 observed at WAIS Divide and the $HO_2 + RO_2$ mixing ratios reported by Bloss et al. (2007) results in an NO_2 concentration of 5 pptv.

The NO_2:NO ratio of 0.26 is significantly lower than the ratios of 0.5–0.75 and 0.71 observed respectively at Halley (Saiz-Lopez et al., 2008; Bauguitte et al., 2012) and Dome C (Frey et al., 2012). These studies showed evidence of large discrepancies between observed and steady-state estimated ratios that are attributed to halogen chemistry for the coastal station, to the presence of HO_2 + RO_2 at Dome C and to snow emissions of mainly NO_2 on the plateau. Therefore it is suggested that the estimated atmospheric NO_2 from the steady-state assumption is a lower limit since a better estimate of the $NO : NO_2$ ratio could be assessed with measurements of mixing ratios of OX and of NO_2 from snow emission at the WAIS Divide site.

4.1.3 Calculation of upper-limit NO_x emission from NO_3^- photolysis

The simplified reaction scheme (R7) to (R10) summarizes the currently known NO_3^- photochemistry in near-surface snow:

$$NO_3^- + h\nu \rightarrow NO_2 + O^- \quad \text{(R7)}$$

$$NO_3^- + h\nu \rightarrow NO_2^- + O(^3P) \quad \text{(R8)}$$

$$NO_2^- + h\nu \rightarrow NO + O^- \quad \text{(R9)}$$

$$NO_2^- + OH \rightarrow NO_2 + OH^- \quad \text{(R10)}$$

ACPD
13, 6807–6849, 2013

Calculations of the NO_2 emission flux from NO_3^- photolysis in snow were based on Reaction (R7) for the wavelengths 290–360 nm (Chu and Anastasio, 2003, and references therein). The first-order rate constant for the photolysis of nitrate at the snowpack surface $j_{NO_3^-,z_0}$ was calculated as defined in Seinfeld and Pandis (1998):

$$j_{NO_3^-,z_0} = \int_{\lambda i}^{\lambda j} \sigma_{NO_3^-}(\lambda,T)\ \phi_{NO_3^-}(\lambda,T)\ I(\lambda,\theta)\ \mathrm{d}\lambda \quad (2)$$

From the results of Chu and Anastasio (2003), the spectral UV absorptivity $\sigma_{NO_3^-}(\lambda)$ was derived between 290 to 360 nm from the measured molar absorption coefficients of aqueous nitrate at 278 K and a quantum yield $\phi_{NO_3^-}(\lambda)$ of 2.79×10^{-3} was estimated for $T = 253$ K. The actinic flux I(λ, θ) were computed with the NCAR/ACD radiative transfer model TUV version 5.0 under clear sky conditions for a 22°solar zenith angle (θ) averaged over the three sampling days.

The transmission of light in snow that drives the photochemistry in the top snowpack is controlled by optical processes: scattering and absorption (Dominé et al., 2008; Grannas et al., 2007, and references therein). These processes are summarized in the parameter *e*-folding depth (EFD), which in turn depends on snow physical properties – grain size, density, liquid water content – and the concentration of light-absorbing impurities such as black carbon.

At Dome C France et al. (2011) measured an EFD of 10 cm for windpacked snow layers containing 1–2 ng g^{-1} of black carbon. Their study showed that absorption in snow layers is function of the black carbon and the HULIS (HUmic LIke Substances) content in snow. While HULIS have not been measured at WAIS Divide, the concentration of black carbon in snow at WAIS Divide is only 10 % of that measured at Concordia station, with an average value of 0.2 ppb measured in the first few meters of the shallow ice core WAIS Divide 05A drilled in 2005 (79.463° S, 112.086° W), 1.5 km distance from our sampling site (J. R. McConnell, personal communication, 2011). Values of $j_{NO_3^-,z_0}$

ACPD
13, 6807–6849, 2013

were then scaled as a function of depth (z) using an EFD of 10, 15 and 20 cm (Table 2):

$$j_{NO_3^-,z} = j_{NO_3^-,z_0} \times \exp\left(\frac{-z}{EFD}\right) \quad (3)$$

The depth-integrated emission flux of NO_2 was calculated for 18 and 28 December 2008 and 4 January 2009 with:

$$F_{NO_2} = \frac{k_{R7}}{k_{R8}} \cdot \int_{z=0\,cm}^{z=30\,cm} [NO_3^-]_z j_{NO_3^-,z}\, dz \quad (4)$$

with a ratio $\frac{k_{R7}}{k_{R8}}$ between 8 and 9 (Grannas et al., 2007, and references therein) and $[NO_3^-]_z$ the concentration of nitrate in molecule cm^{-3} measured at each depth z (Fig. 6).

All of the NO_2 produced from NO_3^- photolysis was assumed to be released from the snowpack. In order to convert flux F_{NO_2} (molecule cm^{-2} s^{-1}) into a volumetric production rate P_{NO_2} (pptv h^{-1}), F_{NO_2} was multiplied with the height of the boundary layer estimated from prior balloon soundings above the West Antarctic Ice Sheet, with a mean (range) of 130 (20–490) m (Frey et al., 2005).

4.1.4 NO_2 production from top snowpack

The resulting potential NO_2 emission fluxes from NO_3^- photolysis in the top surface snowpack were 4.6×10^8–6.6×10^8 molecule cm^{-2} s^{-1} for EFD between 10–20 cm (Table 2). These estimated emissions are in the range of previous values modeled or measured at other Antarctic sites, between 2.4×10^8 and 12.6×10^8 molecule cm^{-2} s^{-1} (Table 3). The result is a local NO_2 production of 1.5 pptv h^{-1} for a boundary layer height of 490 m and 53 pptv h^{-1} for a atmospheric boundary layer depth of 20 m (Table 2). An average production rate of 7 pptv h^{-1} was calculated for a mean BL depth of 130 m (Frey et al., 2005). Comparison between the potential NO_2 production rate and the

ACPD
13, 6807–6849, 2013

mixing ratios of NO_2 estimated from the extended Leighton mechanism (Sect. 4.1.2) indicates that the snow source contributes significantly to the NO_x budget at WAIS Divide.

The above estimates do have uncertainties: first, daily surface snow samplings revealed that the local-scale spatial variability of NO_3^- in the near-surface snowpack is significant. Second, our calculations assume that all of the photo-produced NO_2 is emitted into the atmosphere. The resulting emission fluxes may therefore be an upper limit because: Anastasio and Chu (2009) suggested that 30 % of the NO_2 produced from NO_3^- photolysis may be converted to NO_2^- within the snow matrix before getting released into the atmosphere, production of NO_2 from NO_2^- (Reaction R10) was not calculated since some NO_2^- loss may have occurred during the storage of the samples (Sect. 2.2). And third, these results show the key role of the boundary-layer depth to the contribution of the snowpack emissions to the overlying photochemistry. With an ABL depth ranging from 20 to 490 m observed above WAIS (Frey et al., 2005), our estimate implies that this range of vertical extension of the depth of ABL will impact the atmospheric NO_x mixing ratios rather than the changes in NO_x emission rates from the snowpack. Values of P_{NO_2} suggest also that the estimated production rates are an upper limit since the observed levels of NO and the estimate NO_2 mixing ratio of 5 pptv are inconsistent with a production of 53 pptv h^{-1} for 20-m ABL height.

To further investigate the factors controlling the atmospheric NO_x at WAIS Divide its lifetime was calculated. Assuming that halogen chemistry is not significant at WAIS Divide, Reactions (R11) to (R13) are the main sink of NO_2,:

$$NO_2 + OH + M \rightarrow HNO_3 + M \quad \text{(R11)}$$

$$NO_2 + O_3 \rightarrow NO_3 + O_2 \ (+NO_2 \rightarrow N_2O_5) \quad \text{(R12)}$$

$$NO_2 + HO_2 + M \rightarrow HNO_4 + M \quad \text{(R13)}$$

Based on these reactions and on similar mixing ratios between the photochemical species measured at WAIS Divide and at coastal sites (Sect. 4.1.1), the lifetime of NO_2 (τ_{NO_2}) was estimated with measurements of HO_x at Halley by Bloss et al. (2007)

ACPD
13, 6807–6849, 2013

([OH] = 3.9×10^5 molecule cm^{-3}, [HO_2] = 0.76 pptv). The lifetime of NO_x (τ_{NO_x}) was then deduced through Eq. (5) (Seinfeld and Pandis, 1998):

$$\tau_{NO_x} = \tau_{NO_2} \times \left(1 + \frac{[NO]}{[NO_2]}\right) \quad (5)$$

The resulting lifetime of NO_x at WAIS Divide of 17 h represents an upper limit given that the NO_2 : NO ratio of 0.26 is a lower limit. This value is slightly less than the 24 h estimated by Jones et al. (2000) from a snow block at Neumayer, but it is longer than the 6.4 h estimated at Halley (Bauguitte et al., 2012) and 8 h at South Pole (Davis et al., 2004). Bauguitte et al. (2012) showed that NO_2 lifetime at Halley is mainly controlled by halogen oxidation processes, while low temperatures at South Pole prevent thermal decomposition of pernitric acid and therefore enhance NO_2 removal through its oxidation with HO_2 (Slusher et al., 2002). Thus, our potential NO_x lifetime seems plausible since we expect to observe none of these conditions at WAIS Divide.

Considering a photochemical lifetime of other NO_x precursors, such as HO_2NO_2 and HNO_3, of less than a day above the East Antarctic Plateau (Davis et al., 2008; Slusher et al., 2002) and an air-mass transport between WAIS Divide and the Plateau longer than 17 h (Sect. 4.2), outflows from this region are not expected to be a major NO_x source of the WAIS atmosphere.

4.1.5 Local production of O_3

The main in situ chemical source of tropospheric ozone is its photochemical production through the oxidation of methane. Then Reaction (R1) leads to production of ozone while Reaction (R14) leads to its destruction (Seinfeld and Pandis, 1998):

$$HO_2 + O_3 \rightarrow OH + 2O_2 \quad (R14)$$

ACPD
13, 6807–6849, 2013

The ratio between theses two rates indicates whether WAIS Divide is an ozone production or destruction site:

$$\frac{(R14)}{(R1)} = \frac{k_{R14}}{k_{R1}} \frac{[O_3]}{[NO]} \quad (6)$$

The ratio (R14):(R1) equals 0.216 with $k_{R1} = 9.49 \times 10^{-12}\,cm^3\,molecule^{-1}\,s^{-1}$ and $k_{R14} = 1.62 \times 10^{-15}\,cm^3\,molecule^{-1}\,s^{-1}$, derived from Sander et al. (2006), and an average temperature of 255.6 K measured during the campaign. Even if these calculations are based on a pseudo-steady-state assumption and simplified chemistry, this ratio suggests that WAIS Divide may be a surface-ozone-production site. From Eq. (6), a threshold value of 2 pptv for NO is found to trigger O_3 production whereas this threshold is reached at 5 pptv in the remote continental troposphere (Seinfeld and Pandis, 1998). An atmospheric concentration of HO_2 of 0.76 pptv (Sect. 4.1.4) leads to a potential ozone production of 0.1 ppbv day^{-1}. This is about 1 % of the observed level and 10 % of the rates calculated above the East Antarctic Plateau with $\sim$ 3 ppbv day^{-1} at South Pole (2835 m a.s.l.) (Chen et al., 2004; Crawford et al., 2001) and $\sim$ 1.5 ppbv day^{-1} at the Concordia station (75.06° S, 123.20° E, 3220 m a.s.l.) (Legrand et al., 2009). Our result is however consistent with these previous studies since WAIS Divide is a lower-altitude site with a deeper atmospheric boundary layer that is influenced by a diel cycle of UV irradiance.

It is obvious that local O_3 production is too small to account for the observed increases between 24–25 and 27–29 of December of 0.3 ppbv h^{-1}. We therefore consider the impact of air-mass transport as detailed below.

4.2 Impacts of air-mass transport

Analysis of wind direction and O_3 mixing ratios indicate that air masses from the ENE-SWS sector have typically the highest ozone concentrations (Sect. 2, Fig. 4). O_3 can be considered as a long-lived chemical species compared to NO_x (Sect. 4.1.4) with

ACPD
13, 6807–6849, 2013

a lifetime of 22 days or more in the polar regions (Helmig et al., 2007b; Albert et al., 2002). It is therefore expected that local O_3 is affected by transport, so the origin and transport of air at WAIS Divide were further investigated using 4-day back trajectories.

These trajectories were computed with the NOAA Hysplit model (Draxler and Rolph, 2003. HYSPLIT (HYbrid Single-Particle Lagrangian Integrated Trajectory) http://ready.arl.noaa.gov/hysplit4.html) every 4 h at the altitude of 10 m above the sampling location from 10 December 2008 to 8 January 2009. The resulting 168 back trajectories were combined to create daily maps (Fig. 7) and we distinguish regions of air mass origin by elevation and previous ozone measurements (Fig. 8). Elevated O_3 have not been observed below 2500 m a.m.s.l. during the Antarctic summer (Frey et al., 2005). We therefore refer to the East Antarctic Plateau as the region above 2500 m a.m.s.l., where surface ozone is produced and possibly exported through air outflow (Sect. 4.2.2) Frey et al. (2005) reported an average temperature of about −15 °C below 1750 m a.m.s.l. and of about −25 °C above this elevation. The region below 1750 m a.m.s.l. is then referred as the West Antarctic coast while the interior of WAIS is considered above this elevation.

Figure 8 shows that over the campaign, 41.1 % of the air masses originated from the East Antarctic regions below 2500 m a.m.s.l., 29.7 % was transported from the West Antarctic coastal regions and the inner WAIS, 26.8 % of the air was advected from the East Antarctic Plateau and 2.4 % was flowing from the distant King Haakon VII coast.

4.2.1 Air mass origins related to low O_3 levels

Except for outflows from the East Antarctic Plateau, all air-mass origins are associated with low O_3 averaging 12.8 ± 2.7 ppbv (Fig. 9).

From the 29.7 % of back trajectories that indicate a source from the West Antarctic Ice Sheet, 15.4 % are attributed to West Antarctic coasts (Figs. 7a and 8). West Antarctic coastal air mass originated from four areas: Ross Ice Shelf coast, Weddell Ice shelf coast, Bellingshausen sea coast and Amundsen sea coast. In coastal Antarctica, halogen-catalyzed chemistry has been found to prevent ozone production in summer

ACPD
13, 6807–6849, 2013

and even leads to the well-known episodic ozone depletion events during spring (Bauguitte et al., 2012; Jones et al., 2008; Bloss et al., 2007; Saiz-Lopez et al., 2007). It is therefore thought that coastal air will reduce O_3 levels at WAIS Divide.

Air masses from below the East Antarctic Plateau (41.1 % of all back trajectories, Figs. 7b and 8) and from the interior of WAIS (14.3 % of all back trajectories, Figs. 7e and 8) are also associated with low O_3 mixing ratios. This may indicate that either these regions are influenced by the halogen chemistry from the Antarctic coasts or that halogen chemistry possibly occur at these sites.

Air flows from long-distant sources such as King Haakon VII sea coast (Fig. 7f) appear infrequently, with no obvious impact on local O_3. The ozone signature of these air masses likely disappeared during their transport over more than 2500 km distance.

4.2.2 Air mass origins associated with elevated O_3 levels

26.8 % of all back trajectories point to airflows from the East Antarctic Plateau (Figs. 7c, d and 8) that are mainly related to the highest O_3 measured at WAIS Divide, with an average $\pm 1\sigma$ of 19.4 ± 4.3 ppbv (Fig. 9).

This is consistent with ozone production above the East Antarctic Plateau (Helmig et al., 2008a,b; Crawford et al., 2001) that enhances the O_3 levels of WAIS through air transport, as previously reported by Legrand et al. (2009) who only observed high O_3 mixing ratios at Dumont D'Urville (66.40° S, 140.01° E, 40 m a.m.s.l.) for air masses originating from the Antarctic Plateau. Such oxidizing environment is confirmed by the O_3 observations at South Pole (S. J. Oltmans, http://ds.data.jma.go.jp/gmd/wdcgg) over the same period that show an average concentration of 30.8 ppbv, 17 ppbv more than levels observed at WAIS Divide (Fig. 9).

Further back-trajectory analysis reveals two conditions in which high O_3 concentrations are observed above WAIS Divide. First, elevated O_3 mixing ratios were only observed for air from lower atmosphere coming from the East Antarctic Plateau (below 1500 m above Plateau ground level). The trajectories of these near-surface airflows are in good agreement with the katabatic streamlines described by Parish and Bromwich

ACPD
13, 6807–6849, 2013

(2007). This suggests that air exported off the East Antarctic Plateau via katabatic outflows raises significantly the O_3 mixing ratios at WAIS Divide. The ozone depletion recorded between 25 and 27 December 2008 (Figs. 7d and 9) is attributed to an air mass coming from altitude as high as ~3000 m above Plateau ground level.

Secondly, high O_3 was only observed at WAIS Divide when the transport time from the East Antarctic Plateau was less than 3 days (Fig. 7c, d). To investigate this condition, the total O_3 loss during transport from the Antarctic Plateau to WAIS Divide was estimated. The back trajectories indicate that O_3 maxima during 24–28 December at WAIS Divide are due to rich ozone air originating from the South Pole region as local records show similar but higher peaks about 2 days before (Fig. 9). From this delay, a loss rate of 0.25 (±0.04) ppbv h^{-1} was calculated. This represents an O_3 loss rate of 5.5 (±0.9) ppbv day^{-1} when averaged ozone mixing ratios were respectively 30.1 and 14.0 ppbv at South Pole and WAIS Divide over the campaign. If these loss rates (from dilution, net destruction, etc.) are typical, then it follows that ozone export off the Plateau has to be rapid (< 3 days) in order to have an impact on WAIS Divide's levels.

Observations of elevated O_3 levels are frequently related to vertical transport from the free troposphere/lower stratosphere at Summit (Helmig et al., 2007a, 2002) and other Arctic sites (Helmig et al., 2007b, and references therein). These stratospheric intrusion events are promoted by boundary-layer instabilities, which are caused by significant diurnal radiation cycles and by the size of the Greenland ice sheet (Helmig et al., 2007a). All the vertical O_3 profiles over the East Antarctic Plateau from tethered balloon measurements (Helmig et al., 2008a; Johnson et al., 2008; Oltmans et al., 2008) and airborne study (Slusher et al., 2010) present higher O_3 mixing ratios in the ABL than in the free troposphere, indicating that any contribution of stratospheric ozone occurs over the Antarctic Plateau. Enhancement of the O_3 levels at WAIS Divide from vertical transport is neither supported by the back-trajectory analysis nor by the vertical O_3 profiles measured at South Pole during this period (http://www.esrl.noaa.gov/gmd/dv/data/index.php), confirming the observations from the East Antarctic Plateau.

ACPD
13, 6807–6849, 2013

However, not all elevated O_3 mixing ratios at this site could be explained with the air origin. This is the case of the short ozone peak reaching 23.5 ppbv between 05:00 and 10:00 UTC on 12 December that occurred during the only snowfall precipitation observed during the campaign (Fig. 5).

5 Conclusions

Comparison of local maximum NO_2 production from daily average depth-integrated emission fluxes of NO_2 and the NO_2 mixing ratios estimated from a steady state assumption shows that NO_3^- photolysis in the local snowpack is a significant source of NO_x at WAIS Divide. The upper limit of 17-h NO_x lifetime confirms that short-lived species NO_x are more sensitive to local production above WAIS than outflows from the East Antarctic Plateau.

Calculations of local O_3 production at WAIS Divide point to an air-mass transport contribution rather than a local production. Air masses from the East Antarctic Plateau are only associated with high O_3 mixing ratios if the air transport is near surface by gravity driven winds and less than 3 days from the East Antarctic Plateau. With levels of ozone over the East Antarctic Plateau twice those observed at WAIS Divide, outflows from the interior of the continent have therefore the potential to enhance the mixing ratios of long-lived atmospheric chemical species such as O_3 over WAIS. During this 28-day campaign, outflows from the Antarctic Plateau were observed during 7.5 days, raising the summer O_3 average by 20 % (2 ppbv). Low ozone levels that are associated with air-mass origins from the interior of WAIS raise the possibility of halogen chemistry above inland WAIS that would impact the atmospheric photochemistry.

Results from the back-trajectory analysis over December 2008 and January 2009 at WAIS Divide (Fig. 8) compare well with those of Markle et al. (2012) calculated over thirty years in the Ross Sea region. For the same months, the authors found that 45 % of the air-mass trajectories have an oceanic/West Antarctic origin and 55 % a continental/East Antarctic source, while we observed values of 33 % and 67 % respectively at

ACPD
13, 6807–6849, 2013

WAIS Divide. These results confirm the minor contribution of oceanic/West Antarctic inflows to the WAIS atmosphere during austral summer shown by Nicolas and Bromwich (2011), and the predominance of continental/East Antarctic air masses that may significantly impact the oxidative capacity of the atmosphere above the interior of WAIS.

Acknowledgements. This work was supported by the National Science Foundations Office of Polar Programs (OPP-0636929). We thank G. Huey for the use of the nitric oxide detector. We also thank J. R. McConnell for sharing the black carbon data from the ITASE traverses shallow ice cores, S. J. Oltmans for using his ozone measurements from South Pole, as well as B. Alexander and E. D. Sofen for their insight concerning the EFD and the nitrate photolysis at WAIS Divide.

References

Abbatt, J. P. D., Thomas, J. L., Abrahamsson, K., Boxe, C., Granfors, A., Jones, A. E., King, M. D., Saiz-Lopez, A., Shepson, P. B., Sodeau, J., Toohey, D. W., Toubin, C., von Glasow, R., Wren, S. N., and Yang, X.: Halogen activation via interactions with environmental ice and snow in the polar lower troposphere and other regions, Atmos. Chem. Phys., 12, 6237–6271, doi:10.5194/acp-12-6237-2012, 2012. 6809

Albert, M. R., Grannas, A. M., Bottenheim, J., Shepson, P. B., and Perron, F. E.: Processes and properties of snow-air transfer in the high Arctic with application to interstitial ozone at Alert, Canada, Atmos. Environ., 36, 2779–2787, 2002. 6817, 6826

Anastasio, C. and Chu, L.: Photochemistry of Nitrous Acid (HONO) and Nitrous Acidium Ion (H_2ONO^+) in Aqueous Solution and Ice, Environ. Sci. Technol., 43, 1108–1114, 2009. 6823

Anastasio, C. and Robles, T.: Light absorption by soluble chemical species in Arctic and Antarctic snow, J. Geophys. Res.-Atmos., 112, D24304, doi:10.1029/2007JD008695, 2007. 6818

Bales, R. C., Mcconnell, J. R., Losleben, M. V., Conklin, M. H., Fuhrer, K., Neftel, A., Dibb, J. E., Kahl, J. D. W., and Stearns, C. R.: Diel variations of H_2O_2 in Greenland: a discussion of the cause and effect relationship, J. Geophys. Res., 100, 18661–18668, 1995. 6817

Banta, J. R., Mcconnell, J. R., Frey, M. M., Bales, R. C., and Taylor, K.: Spatial and temporal variability in snow accumulation at the West Antarctic Ice Sheet Divide over recent centuries, J. Geophys. Res., 113, 1–8, 2008. 6815

ACPD
13, 6807–6849, 2013

Bauguitte, S. J.-B., Brough, N., Frey, M. M., Jones, A. E., Maxfield, D. J., Roscoe, H. K., Rose, M. C., and Wolff, E. W.: A network of autonomous surface ozone monitors in Antarctica: technical description and first results, Atmos. Meas. Tech., 4, 645–658, doi:10.5194/amt-4-645-2011, 2011. 6812

Bauguitte, S. J.-B., Bloss, W. J., Evans, M. J., Salmon, R. A., Anderson, P. S., Jones, A. E., Lee, J. D., Saiz-Lopez, A., Roscoe, H. K., Wolff, E. W., and Plane, J. M. C.: Summertime NO_x measurements during the CHABLIS campaign: can source and sink estimates unravel observed diurnal cycles?, Atmos. Chem. Phys., 12, 989–1002, doi:10.5194/acp-12-989-2012, 2012. 6809, 6820, 6824, 6827, 6840

Bloss, W. J., Lee, J. D., Heard, D. E., Salmon, R. A., Bauguitte, S. J.-B., Roscoe, H. K., and Jones, A. E.: Observations of OH and HO_2 radicals in coastal Antarctica, Atmos. Chem. Phys., 7, 4171–4185, doi:10.5194/acp-7-4171-2007, 2007. 6820, 6823, 6827

Chen, G., Davis, D. D., Crawford, J. H., Hutterli, M. A., Huey, G., Slusher, D., Mauldin, L., Eisele, F., Tanner, D., Dibb, J. E., Buhr, M., Mcconnell, J. R., Lefer, B., Shetter, R., Blake, D. R., Song, C., Lombardi, K., and Arnoldy, J.: A reassessment of HO_x South Pole chemistry based on observations recorded during ISCAT 2000, Atmos. Environ., 38, 5451–5461, 2004. 6810, 6825

Chu, L. and Anastasio, C.: Quantum yields of hydroxyl radical and nitrogen dioxide from the photolysis of nitrate on ice, J. Phys. Chem. A, 107, 9594–9602, 2003. 6821

Crawford, J. H., Davis, D. D., Chen, G., Buhr, M., Oltmans, S., Weller, R., Mauldin, L., Eisele, F., Shetter, R., Lefer, B., Arimoto, R., and Hogan, A.: Evidence for photochemical production of ozone at the South Pole surface, Geophys. Res. Lett., 28, 3641–3644, 2001. 6810, 6825, 6827

Davis, D. D., Nowak, J., Chen, G., Buhr, M., Arimoto, R., Hogan, A., Eisele, F., Mauldin, L., Tanner, D., Shetter, R., Lefer, B., and McMurry, P.: Unexpected high levels of NO observed at South Pole, Geophys. Res. Lett., 28, 3625–3628, 2001. 6811

Davis, D. D., Chen, G., Buhr, M., Crawford, J. H., Lenschow, D., Lefer, B., Shetter, R., Eisele, F., Mauldin, L., and Hogan, A.: South Pole NO_x chemistry: an assessment of factors controlling variability and absolute levels, Atmos. Environ., 38, 5375–5388, 2004. 6810, 6811, 6824, 6843

Davis, D. D., Seelig, J., Huey, G., Crawford, J. H., Chen, G., Wang, Y., Buhr, M., Helmig, D., Neff, W., Blake, D. R., Arimoto, R., and Eisele, F.: A reassessment of Antarctic plateau

ACPD
13, 6807–6849, 2013

reactive nitrogen based on ANTO 2003 airborne and ground based measurements, Atmos. Environ., 42, 2831–2848, 2008. 6809, 6824

Dibb, J. E., Huey, G., Slusher, D., and Tanner, D.: Soluble reactive nitrogen oxides at South Pole during ISCAT 2000, Atmos. Environ., 38, 5399–5409, 2004. 6816, 6843

Domine, F., Albert, M., Huthwelker, T., Jacobi, H.-W., Kokhanovsky, A. A., Lehning, M., Picard, G., and Simpson, W. R.: Snow physics as relevant to snow photochemistry, Atmos. Chem. Phys., 8, 171–208, doi:10.5194/acp-8-171-2008, 2008. 6821

Eisele, F. L. and Davis, D. D.: Antarctic tropospheric chemistry investigation (ANTCI) 2003, Atmos. Environ., 42, 2747–2748, 2008. 6810

France, J. L., King, M. D., Frey, M. M., Erbland, J., Picard, G., Preunkert, S., MacArthur, A., and Savarino, J.: Snow optical properties at Dome C (Concordia), Antarctica; implications for snow emissions and snow chemistry of reactive nitrogen, Atmos. Chem. Phys., 11, 9787–9801, doi:10.5194/acp-11-9787-2011, 2011. 6812, 6816, 6819, 6821, 6840

Frey, M. M., Stewart, R. W., Mcconnell, J. R., and Bales, R. C.: Atmospheric hydroperoxides in West Antarctica: links to stratospheric ozone and atmospheric oxidation capacity, J. Geophys. Res., 110, 1–17, 2005. 6810, 6812, 6814, 6816, 6818, 6822, 6823, 6826, 6838, 6843

Frey, M. M., Bales, R. C., and Mcconnell, J. R.: Climate sensitivity of the century-scale hydrogen peroxide (H_2O_2) record preserved in 23 ice cores from West Antarctica, J. Geophys. Res.-Atmos., 111, D21301, doi:10.1029/2005JD006816, 2006. 6810, 6813

Frey, M. M., Hutterli, M. A., Chen, G., Sjostedt, S. J., Burkhart, J. F., Friel, D. K., and Bales, R. C.: Contrasting atmospheric boundary layer chemistry of methylhydroperoxide (CH_3OOH) and hydrogen peroxide (H_2O_2) above polar snow, Atmos. Chem. Phys., 9, 3261–3276, doi:10.5194/acp-9-3261-2009, 2009a. 6812, 6816, 6817, 6818, 6843

Frey, M. M., Savarino, J., Morin, S., Erbland, J., and Martins, J. M. F.: Photolysis imprint in the nitrate stable isotope signal in snow and atmosphere of East Antarctica and implications for reactive nitrogen cycling, Atmos. Chem. Phys., 9, 8681–8696, doi:10.5194/acp-9-8681-2009, 2009b. 6809

Frey, M. M., Brough, N., France, J. L., Traulle, O., Anderson, P. S., King, M. D., Jones, A. E., Wolff, E. W., and Savarino, J.: The diurnal variability of atmospheric nitrogen oxides (NO and NO_2) above the Antarctic Plateau driven by atmospheric stability and snow emissions, Atmos. Chem. Phys. Discuss., 12, 22309–22353, doi:10.5194/acpd-12-22309-2012, 2012. 6809, 6817, 6819, 6820, 6840, 6843

ACPD
13, 6807–6849, 2013

Grannas, A. M., Jones, A. E., Dibb, J., Ammann, M., Anastasio, C., Beine, H. J., Bergin, M., Bottenheim, J., Boxe, C. S., Carver, G., Chen, G., Crawford, J. H., Dominé, F., Frey, M. M., Guzmán, M. I., Heard, D. E., Helmig, D., Hoffmann, M. R., Honrath, R. E., Huey, L. G., Hutterli, M., Jacobi, H. W., Klán, P., Lefer, B., McConnell, J., Plane, J., Sander, R., Savarino, J., Shepson, P. B., Simpson, W. R., Sodeau, J. R., von Glasow, R., Weller, R., Wolff, E. W., and Zhu, T.: An overview of snow photochemistry: evidence, mechanisms and impacts, Atmos. Chem. Phys., 7, 4329.-4373, doi:10.5194/acp-7-4329-2007, 2007. 6809, 6821, 6822

Helmig, D., Boulter, J., David, D., Birks, J., Cullen, N., Steffen, K., Johnson, B., and Oltmans, S. J.: Ozone and meteorological Summit, Greenland, boundary-layer conditions at during 3–21 June 2000, Atmos. Environ., 36, 2595–2608, 2002. 6828

Helmig, D., Bocquet, F., Cohen, L., and Oltmans, S. J.: Ozone uptake to the polar snowpack at Summit, Greenland, Atmos. Environ., 41, 5061–5076, 2007a. 6828

Helmig, D., Oltmans, S. J., Carlson, D., Lamarque, J.-F., Jones, A. E., Labuschagne, C., Anlauf, K., and Hayden, K.: A review of surface ozone in the polar regions, Atmos. Environ., 41, 5138–5161, 2007b. 6817, 6826, 6828

Helmig, D., Johnson, B., Oltmans, S. J., Neff, W., Eisele, F., and Davis, D. D.: Elevated ozone in the boundary layer at South Pole, Atmos. Environ., 42, 2788–2803, 2008a. 6810, 6827, 6828

Helmig, D., Johnson, B., Warshawsky, M., Morse, T., Neff, W., Eisele, F., and Davis, D. D.: Nitric oxide in the boundary-layer at South Pole during the Antarctic Tropospheric Chemistry Investigation (ANTCI), Atmos. Environ., 42, 2817–2830, 2008b. 6810, 6827

Honrath, R., Peterson, M., Guo, S., Dibb, J., Shepson, P., and Campbell, B.: Evidence of NO_x production within or upon ice particles in the Greenland snowpack, Geophys. Res. Lett., 26, 695–698, 1999. 6809

Hutterli, M. A., Mcconnell, J. R., Stewart, R. W., Jacobi, H.-W., and Bales, R. C.: Impact of temperature-driven cycling of hydrogen peroxide (H_2O_2) between air and snow on the planetary boundary layer, J. Geophys. Res.-Atmos., 106, 15395–15404, 2001. 6817

Hutterli, M. A., Mcconnell, J. R., Chen, G., Bales, R. C., Davis, D. D., and Lenschow, D.: Formaldehyde and hydrogen peroxide in air, snow and interstitial air at South Pole, Atmos. Environ., 38, 5439–5450, 2004. 6817

Jacobi, H.-W., Weller, R., Jones, A. E., Anderson, P. S., and Schrems, O.: Peroxyacetyl nitrate (PAN) concentrations in the Antarctic troposphere measured during the photochemical experiment at Neumayer (PEAN'99), Atmos. Environ., 34, 5235–5247, 2000. 6843

ACPD
13, 6807–6849, 2013

Jarvis, J. C., Hastings, M. G., Steig, E. J., and Kunasek, S. A.: Isotopic ratios in gas-phase HNO_3 and snow nitrate at Summit, Greenland, J. Geophys. Res., 114, D17301, doi:10.1029/2009JD012134, 2009. 6818

Jefferson, A., Tanner, D., Eisele, F., Davis, D., Chen, G., Crawford, J., Huey, J., Torres, A., and Berresheim, H.: OH photochemistry and methane sulfonic acid formation in the coastal Antarctic boundary layer, J. Geophys. Res.-Atmos, 103, 1647–1656, 1998. 6843

Johnson, B., Helmig, D., and Oltmans, S. J.: Evaluation of ozone measurements from a tethered balloon-sampling platform at South Pole Station in December 2003, Atmos. Environ., 42, 2780–2787, 2008. 6828

Jones, A., Weller, R., Minikin, A., Wolff, E., Sturges, W., McIntyre, H., Leonard, S., Schrems, O., and Bauguitte, S.: Oxidized nitrogen chemistry and speciation in the Antarctic troposphere, J. Geophys. Res.-Atmos., 104, 21355–21366, 1999. 6843

Jones, A., Weller, R., Anderson, P., Jacobi, H., Wolff, E., Schrems, O., and Miller, H.: Measurements of NO_x emissions from the Antarctic snowpack, Geophys. Res. Lett., 28, 1499–1502, 2001. 6840

Jones, A. E., Weller, R., Wolff, E. W., and Jacobi, H.-W.: Speciation and rate of photochemical NO and NO_2 production in Antarctic snow, Geophys. Res. Lett., 27, 345–348, 2000. 6809, 6824

Jones, A. E., Wolff, E. W., Salmon, R. A., Bauguitte, S. J.-B., Roscoe, H. K., Anderson, P. S., Ames, D., Clemitshaw, K. C., Fleming, Z. L., Bloss, W. J., Heard, D. E., Lee, J. D., Read, K. A., Hamer, P., Shallcross, D. E., Jackson, A. V., Walker, S. L., Lewis, A. C., Mills, G. P., Plane, J. M. C., Saiz-Lopez, A., Sturges, W. T., and Worton, D. R.: Chemistry of the Antarctic Boundary Layer and the Interface with Snow: an overview of the CHABLIS campaign, Atmos. Chem. Phys., 8, 3789–3803, doi:10.5194/acp-8-3789-2008, 2008. 6827

Jones, A. E., Wolff, E. W., Ames, D., Bauguitte, S. J.-B., Clemitshaw, K. C., Fleming, Z., Mills, G. P., Saiz-Lopez, A., Salmon, R. A., Sturges, W. T., and Worton, D. R.: The multi-seasonal NO_y budget in coastal Antarctica and its link with surface snow and ice core nitrate: results from the CHABLIS campaign, Atmos. Chem. Phys., 11, 9271–9285, doi:10.5194/acp-11-9271-2011, 2011. 6840

Kreutz, K. J., Mayewski, P. A., Twickler, M. S., Whitlow, S. I., White, J., Shuman, C. A., Raymond, C. F., Conway, H., and McConnell, J. R.: Seasonal variations of glaciochemical, isotopic and stratigraphic properties in Siple Dome (Antarctica) surface snow, Ann. Glaciol., 29, 38–44, 1999. 6818

ACPD
13, 6807–6849, 2013

Lee-Taylor, J. and Madronich, S.: Calculation of actinic fluxes with a coupled atmosphere-snow radiative transfer model, J. Geophys. Res.-Atmos., 107(D24), 4796, doi:10.1029/2002JD002084, 2002. 6820

Legrand, M., Preunkert, S., Jourdain, B., Gallée, H., Goutail, F., Weller, R., and Savarino, J.: Year-round record of surface ozone at coastal (Dumont d'Urville) and inland (Concordia) sites in East Antarctica, J. Geophys. Res., 114, D20306, doi:10.1029/2008JD011667, 2009. 6810, 6825, 6827, 6843

Lind, J. A. and Kok, G. L.: Correction to Henry's law determinations for aqueous solutions of hydrogen peroxide, methylhydroperoxide, and peroxyacetic acid, J. Geophys. Res., 99, 21119–21119, 1994. 6818

Markle, B. R., Bertler, N. A. N., Sinclair, K. E., and Sneed, S. B.: Synoptic variability in the Ross Sea region, Antarctica, as seen from back-trajectory modeling and ice core analysis, J. Geophys. Res., 117, D02113, doi:10.1029/2011JD016437, 2012. 6829

Mauldin, L., Kosciuch, E., Henry, B., Eisele, F., Shetter, R., Lefer, B., Chen, G., Davis, D. D., Huey, G., and Tanner, D.: Measurements of OH, $HO_2 + RO_2$, H_2SO_4, and MSA at the South Pole during ISCAT 2000, Atmos. Environ., 38, 5423–5437, 2004. 6810

Mulvaney, R., Wagenbach, D., and Wolff, E. W.: Postdepositional change in snowpack nitrate from observation of year-round near-surface snow in coastal Antarctica, J. Geophys. Res.-Atmos., 103, 11021–11031, 1998. 6816, 6843

Nicolas, J. P. and Bromwich, D. H.: Climate of West Antarctica and Influence of Marine Air Intrusions, J. Climate, 24, 49–67, 2011. 6830

O'Driscoll, P., Minogue, N., Takenaka, N., and Sodeau, J.: Release of nitric oxide and iodine to the atmosphere from the freezing of sea-salt aerosol components, J. Phys. Chem. A, 112, 1677–1682, 2012. 6813

Oltmans, S. J., Johnson, B. J., and Helmig, D.: Episodes of high surface-ozone amounts at South Pole during summer and their impact on the long-term surface-ozone variation, Atmos. Environ., 42, 2804–2816, 2008. 6828

Oncley, S., Buhr, M., Lenschow, D., Davis, D., and Semmer, S.: Observations of summertime NO fluxes and boundary-layer height at the South Pole during ISCAT 2000 using scalar similarity, Atmos. Environ., 38, 5389–5398, 2004. 6840

Parish, T. R. and Bromwich, D. H.: Reexamination of the near-surface airflow over the Antarctic continent and implications on atmospheric circulations at high southern latitudes, Mon. Weather Rev., 135, 1961–1973, 2007. 6827

ACPD
13, 6807–6849, 2013

Preunkert, S., Ancellet, G., Legrand, M., Kukui, A., Kerbrat, M., Sarda-Estève, R., Gros, V., and Jourdain, B.: Oxidant production over Antarctic Land and its export (OPALE) project: an overview of the 2010–2011 summer campaign, J. Geophys. Res., 117, D15307, doi:10.1029/2011JD017145, 2012. 6843

Ridley, B., Walega, J., Montzka, D., Grahek, F., Atlas, E., Flocke, F., Stroud, V., Deary, J., Gallant, A., Boudries, H., Bottenheim, J., Anlauf, K., Worthy, D., Sumner, A., Splawn, B., and Shepson, P.: Is the Arctic surface layer a source and sink of NO_x in winter/spring?, J. Atmos. Chem., 36, 1–22, 2000. 6819, 6820

Rothlisberger, R., Hutterli, M., Sommer, S., Wolff, E., and Mulvaney, R.: Factors controlling nitrate in ice cores: Evidence from the Dome C deep ice core, J. Geophys. Res.-Atmos., 105, 20565–20572, 2000. 6816, 6843

Saiz-Lopez, A., Mahajan, A. S., Salmon, R. A., Bauguitte, S. J. B., Jones, A. E., Roscoe, H. K., and Plane, J. M. C.: Boundary layer halogens in coastal Antarctica, Science, 317, 348–351, 2007. 6827

Saiz-Lopez, A., Plane, J. M. C., Mahajan, A. S., Anderson, P. S., Bauguitte, S. J.-B., Jones, A. E., Roscoe, H. K., Salmon, R. A., Bloss, W. J., Lee, J. D., and Heard, D. E.: On the vertical distribution of boundary layer halogens over coastal Antarctica: implications for O_3, HO_x, NO_x and the Hg lifetime, Atmos. Chem. Phys., 8, 887–900, doi:10.5194/acp-8-887-2008, 2008. 6820

Sander, S. P., Finlayson-Pitts, B. J., Friedl, R. R., Golden, D. M., Huie, R. E., Keller-Rudek, H., Kolb, C. E., Kurylo, M. J., Molina, M. J., Moortgat, G. K., Orkin, V. L., Ravishankara, A. R., and Wine, P. H: Chemical kinetics and photochemical data for use in atmospheric studies, Evaluation number 15, JPL Publication 06-2, Jet Propulsion Laboratory, Pasadena, 2006. 6820, 6825

Seinfeld, J. H. and Pandis, S. N.: Atmospheric Chemistry and Physics: From Air Pollution to Climate Change, John Wiley & Sons, Inc., 1998. 6821, 6824, 6825

Slusher, D., Huey, G., Tanner, D., Chen, G., Davis, D. D., Buhr, M., Nowak, J., Eisele, F., Kosciuch, E., Mauldin, L., Lefer, B., Shetter, R., and Dibb, J. E.: Measurements of pernitric acid at the South Pole during ISCAT 2000, Geophys. Res. Lett., 29(21), 2011, doi:10.1029/2002GL015703, 2002. 6824

Slusher, D. L., Neff, W. D., Kim, S., Huey, L. G., Wang, Y., Zeng, T., Tanner, D. J., Blake, D. R., Beyersdorf, A., Lefer, B. L., Crawford, J. H., Eisele, F. L., Mauldin, R. L., Kosciuch, E., Buhr, M. P., Wallace, H. W., and Davis, D. D.: Atmospheric chemistry results from the

ACPD
13, 6807–6849, 2013

ANTCI 2005 Antarctic plateau airborne study, J. Geophys. Res.-Atmos., 115, D07304, doi:10.1029/2009JD012605, 2010. 6809, 6810, 6828

Takenaka, N. and Bandow, H.: Chemical kinetics of reactions in the unfrozen solution of ice, J. Phys. Chem. A, 111, 8780–8786, 2007. 6813

Thomas, J. L., Stutz, J., Lefer, B., Huey, L. G., Toyota, K., Dibb, J. E., and von Glasow, R.: Modeling chemistry in and above snow at Summit, Greenland – Part 1: Model description and results, Atmos. Chem. Phys., 11, 4899–4914, doi:10.5194/acp-11-4899-2011, 2011. 6816

Thomas, J. L., Dibb, J. E., Huey, L. G., Liao, J., Tanner, D., Lefer, B., von Glasow, R., and Stutz, J.: Modeling chemistry in and above snow at Summit, Greenland – Part 2: Impact of snowpack chemistry on the oxidation capacity of the boundary layer, Atmos. Chem. Phys., 12, 6537–6554, doi:10.5194/acp-12-6537-2012, 2012. 6809

Traversi, R., Becagli, S., Castellano, E., Cerri, O., Morganti, A., Severi, M., and Udisti, R.: Study of Dome C site (East Antartica) variability by comparing chemical stratigraphies, Microchem. J., 92, 7–14, 2009. 6816

Wang, Y., Choi, Y., Zeng, T., Davis, D., Buhr, M., Huey, L. G., and Neff, W.: Assessing the photochemical impact of snow NO_x emissions over Antarctica during ANTCI 2003, Atmos. Environ., 42, 2849–2863, 2008. 6840

Wolff, E. W., Jones, A. E., Bauguitte, S. J.-B., and Salmon, R. A.: The interpretation of spikes and trends in concentration of nitrate in polar ice cores, based on evidence from snow and atmospheric measurements, Atmos. Chem. Phys., 8, 5627–5634, doi:10.5194/acp-8-5627-2008, 2008. 6818

ACPD
13, 6807–6849, 2013

Table 1. Averages $\pm 1\sigma$ (medians) of atmospheric and snow concentrations of the chemical species observed at WAIS Divide and nearby sites.

Site	atmospheric				snow		
	NO (pptv)	O_3 (ppbv)	H_2O_2 (pptv)	MHP (pptv)	H_2O_2 (ppbw)	NO_3^- (ppbw)	NO_2^- (ppbw)
WAIS Divide	19 ± 31 (10)	14 ± 4 (13)	743 ± 362 (695)	519 ± 238 (464)	238 ± 37 (238)	137 ± 37 (142)	0.6 ± 0.4 (0.5)
ITASE 00-1[a]	–	–	303 ± 159	–	175	–	–
Byrd[b]	10	20 ± 2	364 ± 138	422 ± 162	33 ± 9	–	–
	–	(20)	(348)	(411)	(34)	–	–

[a] 79.38° S, 111.23° W, 1791 m a.m.s.l.

[b] 80.02° S, 119.60° W, 1537 m a.m.s.l.; NO based on optimum model runs (Frey et al., 2005); atmospheric H_2O_2 from sampling at site RIDS-C (80.00° S, 119.53° W, 1575 m a.m.s.l.); H_2O_2 in snow from sampling at site RIDS-B in 1996 (79.46° S, 118.04° W, 1650 m a.m.s.l.)

ACPD
13, 6807–6849, 2013

Table 2. Potential emission fluxes of NO_2 (F_{NO_2}) from NO_3^- photolysis. Results of NO_2^- production ($P_{NO_2^-}$) and NO_2 production (P_{NO_2}) represent averaged values from estimations based on a ratio Reaction (R7) : (R8) of 8 : 1 and of 9 : 1.

EFD (cm)	F_{NO_2} (10^8 molecule cm^{-2} s^{-1})	$P_{NO_2^-}$ (pptv h^{-1})	P_{NO_2} (pptv h^{-1})		
			ABL = 130	ABL = 20	ABL = 490
10	4.57	288	5.5	36.6	1.5
15	5.74	362	7.0	46.0	1.9
20	6.59	416	8.0	52.8	2.2

ACPD
13, 6807–6849, 2013

Table 3. Potential emission fluxes of NO_x from nitrate photolysis at WAIS Divide in comparison to prior calculated or measured NO_x rates from other Antarctic sites.

Site and reference	$F_{NO_x} \pm 1\sigma$ (10^8 molecule cm^{-2} s^{-1}) Measured	Modeled	Period	Notes
Neumayer:				
Jones et al. (2001)	3(+0.3/ − 0.9)[a]		5–7 Feb 1999	Noon maxima
Halley V:				
Jones et al. (2011)	2.42[b]		18 Jan 2005	Daily average
Bauguitte et al. (2012)	12.6[a]	3.48[c]	2 Feb 2005	Noon maxima
	7.3[a]			(07:05–15:05 UTC) average
South Pole:				
Wang et al. (2008)		3.2–4.2[d]	Nov–Dec 2003	
Oncley et al. (2004)	3.9 ± 0.4[e]		26–30 Nov 2000	Overall average
Dome C:				
Frey et al. (2012)		6.9 ± 7.2[a]	Dec 2009–Jan 2010	
South Pole:				
Oncley et al. (2004)	F_{NO} = 2.6 ± 0.3		26–30 Nov 2000	Overall average
Dome C:				
France et al. (2011)		F_{NO_2} = 2.4–3.8[f]	Dec 2009–Jan 2010	Values for 22° SEA
WAIS Divide:				
This study	F_{NO_2} = 4.6–6.6[b]		Dec 2008–Jan 2009	Daily average, 22° SEA

[a] from measured gradients NO_x concentrations and turbulent diffusivity
[b] depth-integrated F_{NO_x} with spectral irradiance from the TUV model
[c] from 1-D model of NO_x concentrations based on production from NO_3^- photolysis and chemical loss
[d] from 1-D chemistry-diffusion model based on trace gas measurements
[e] based on observed NO gradients and assuming photochemical steady-state
[f] depth-integrated F_{NO_x} with measured spectral irradiance

ACPD
13, 6807–6849, 2013

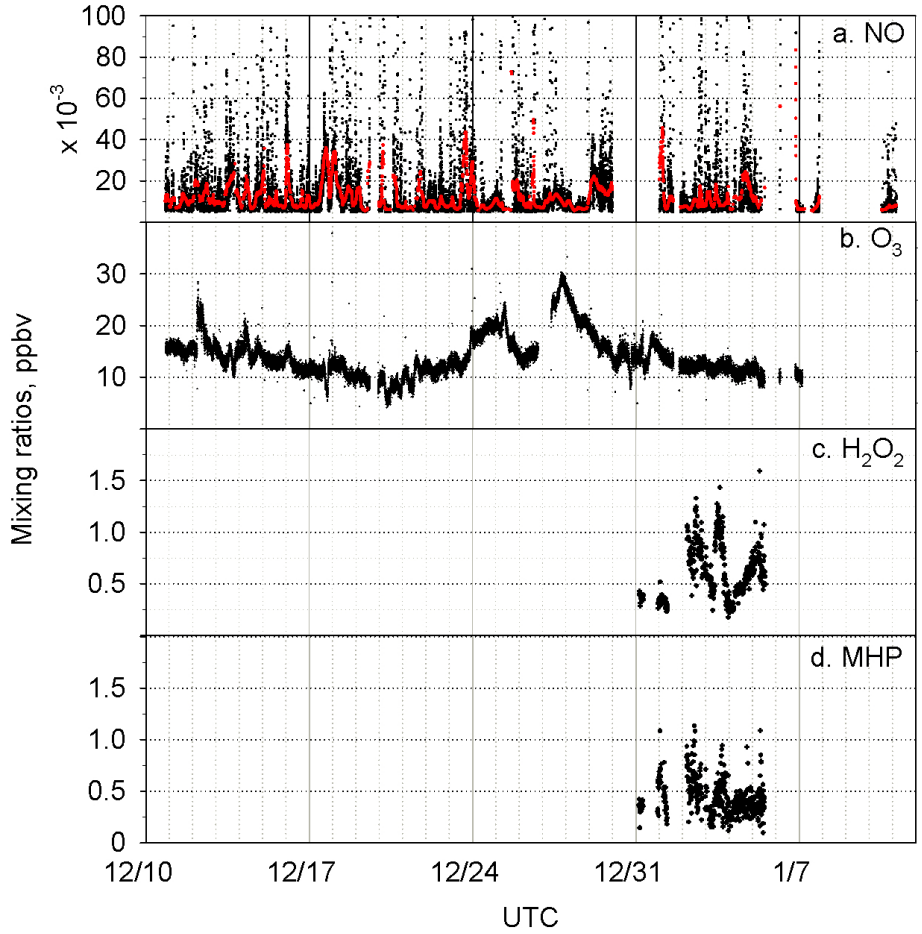

Fig. 1. Atmospheric mixing ratios of NO, O_3 (1-min averages) and of H_2O_2 and MHP (10-min averages) during austral summer 2008–2009 at WAIS Divide. The 4-h running median of NO is shown for comparison (red symbols).

ACPD
13, 6807–6849, 2013

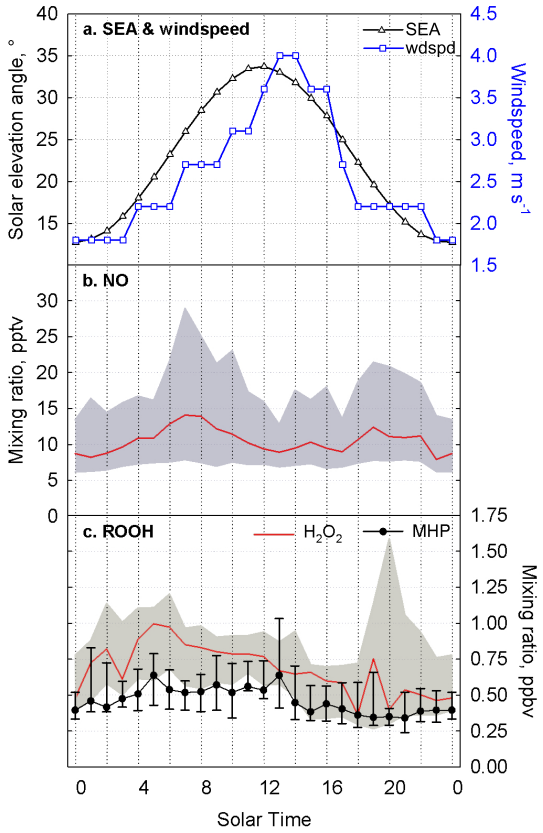

Fig. 2. Diel variation of **(a)** average solar elevation angle and wind speed, **(b)** NO medians, **(c)** H_2O_2 and MHP medians. Symbols are 1-h binned centered on each hour, shaded area and error bars indicating the range between first and third quartiles.

ACPD
13, 6807–6849, 2013

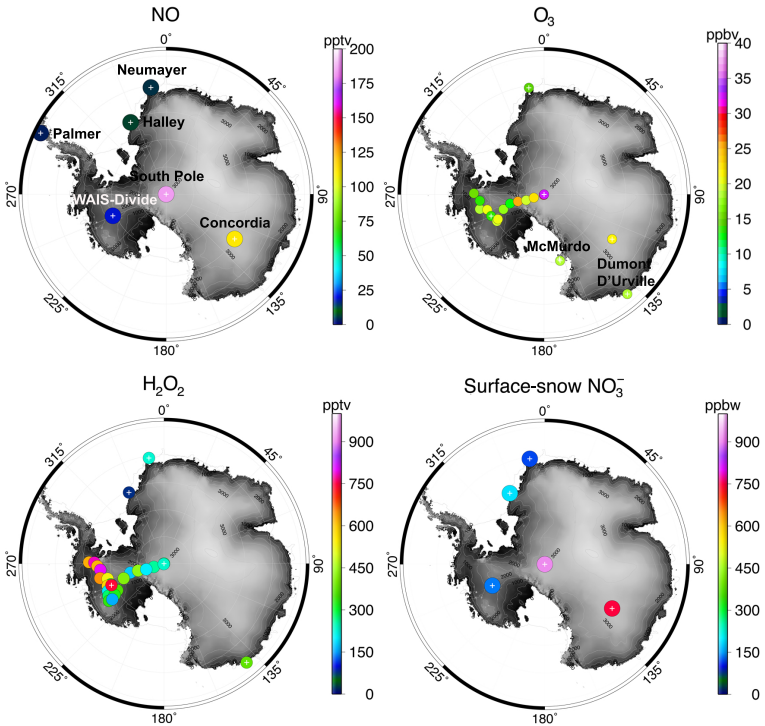

Fig. 3. Report of some previous Antarctic measurements of atmospheric nitric oxide, surface ozone, hydrogen peroxide, plus nitrate in surface snow. Data from: Frey et al. (2012), Preunkert et al. (2012), Frey et al. (2009a), Legrand et al. (2009), Frey et al. (2005), Dibb et al. (2004), Davis et al. (2004), Rothlisberger et al. (2000), Jacobi et al. (2000), Jones et al. (1999), Mulvaney et al. (1998), Jefferson et al. (1998), NOAA/GMD and AWI (http://ds.data.jma.go.jp/gmd/wdcgg/).

ACPD
13, 6807–6849, 2013

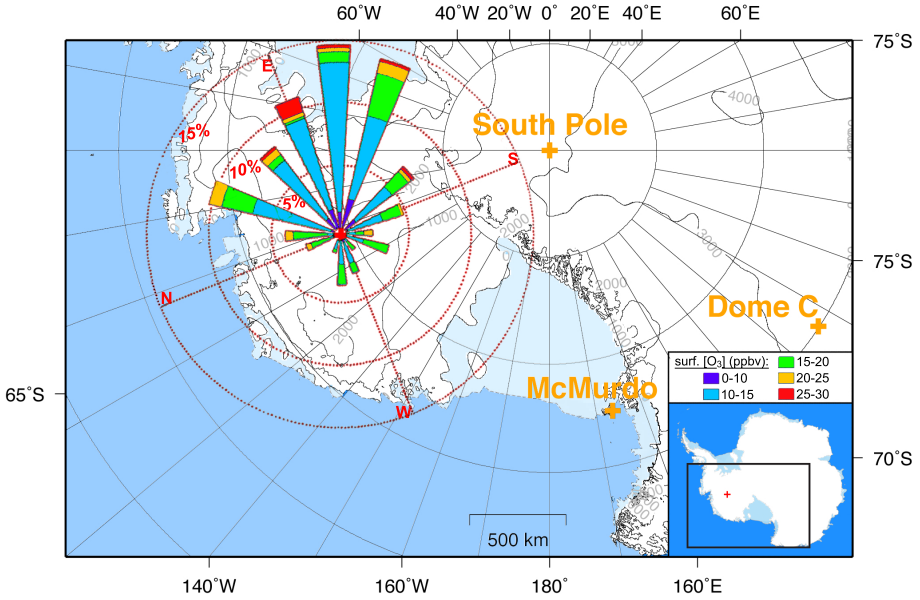

Fig. 4. The windrose analysis at WAIS Divide shows that in two thirds of all cases the wind originates from ENE to SWS, coincident with the highest O_3 mixing ratios detected.

ACPD
13, 6807–6849, 2013

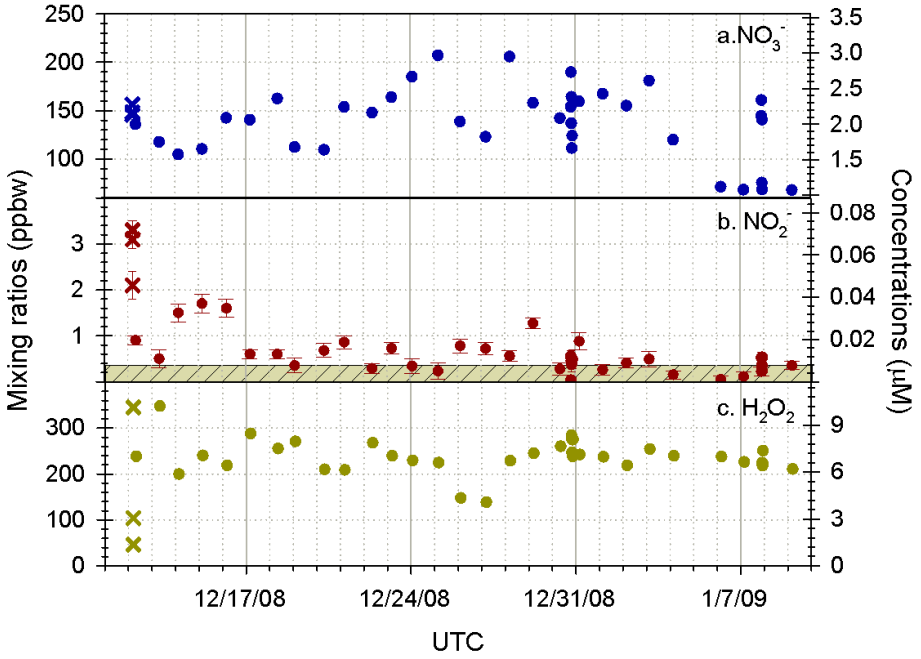

Fig. 5. Surface snow concentrations and snow concentrations from the 12 December 2008 precipitation of **(a)** NO_3^-, **(b)** NO_2^-, **(c)** H_2O_2. The green shaded area represents the NO_2^- LOD.

ACPD
13, 6807–6849, 2013

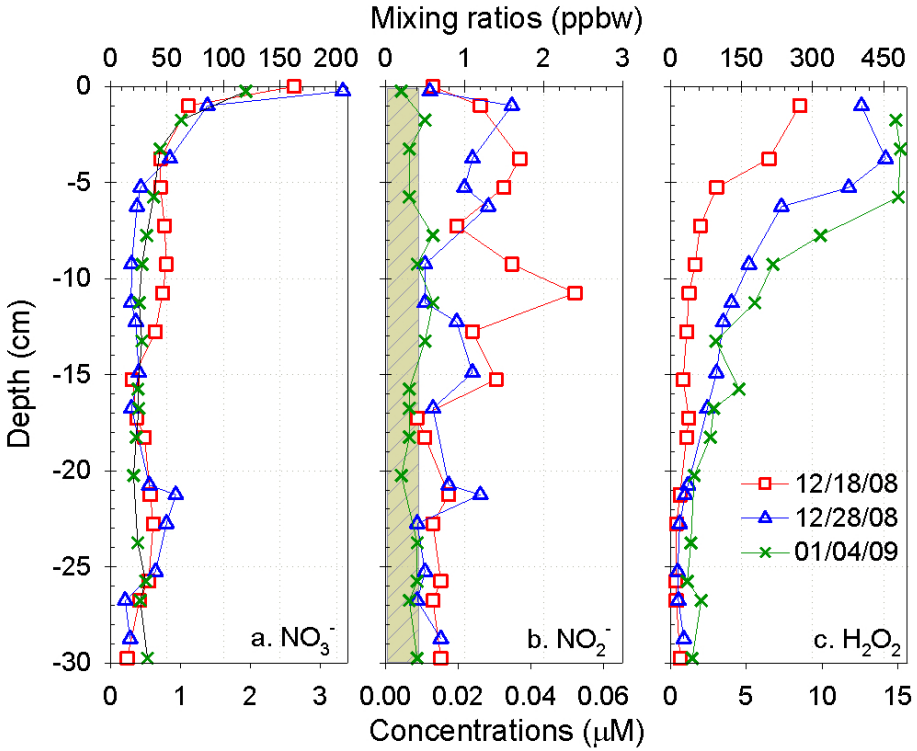

Fig. 6. Snow concentrations of **(a)** NO_3^-, **(b)** NO_2^- and **(c)** H_2O_2 measured in the 30 cm-depth snow pits dug on 18 December 2008 (red squares), 28 December 2008 (blue triangles) and 4 January 2009 (green crosses). The green shaded area represents the NO_2^- LOD.

ACPD
13, 6807–6849, 2013

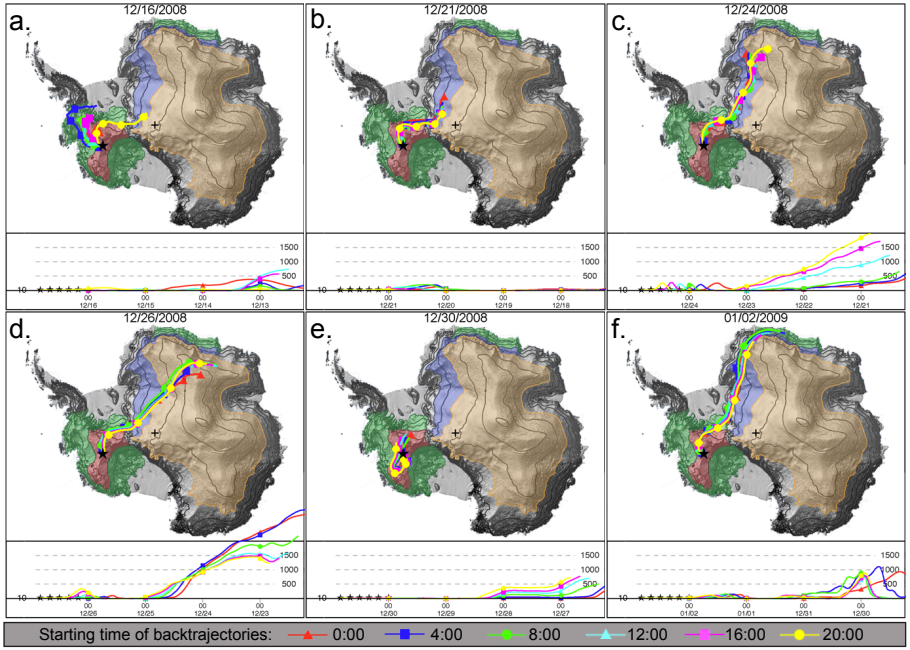

Fig. 7. Combined 4-day back trajectories maps of some specific events identified in Fig. 9. Each daily map contain 6 trajectories of 4 h interval and symbols are plotted for every 24 h step time. The different regions of air origin are: East Antarctic Plateau (yellow), regions below East Antarctic Plateau (blue), WAIS (red) and Antarctic coast (green).

ACPD
13, 6807–6849, 2013

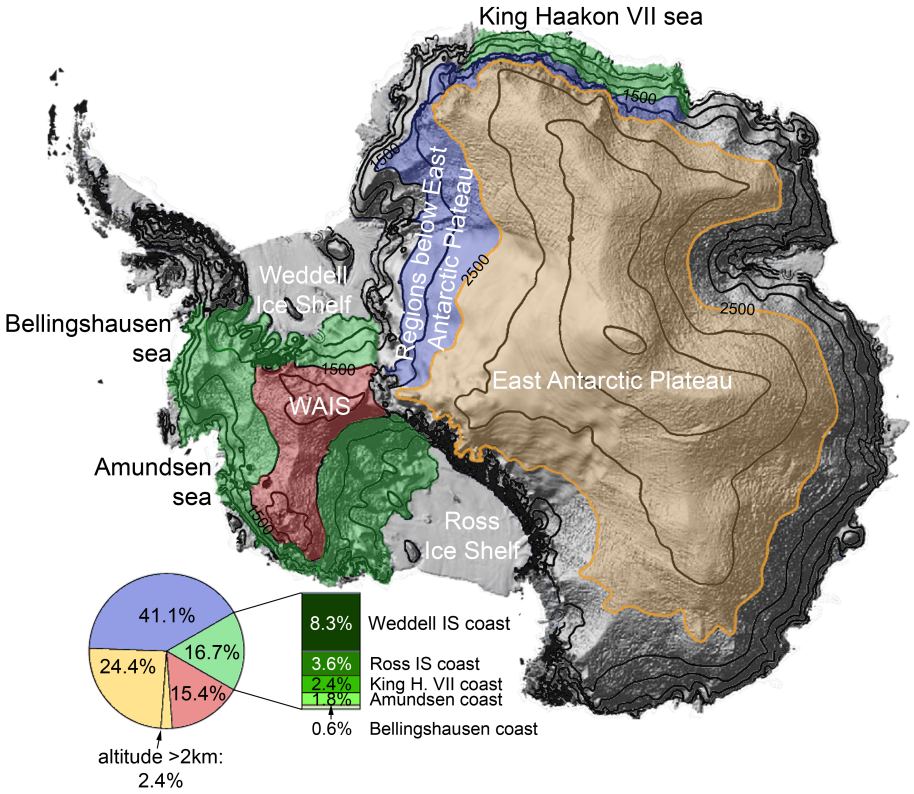

Fig. 8. Map of the different origins of the air reaching WAIS Divide identified on the 4-day back trajectory analysis and topography: East Antarctic Plateau (yellow), regions below East Antarctic Plateau (blue), WAIS (red) and the coast (green): Amundsen sea coast, Bellingshausen sea coast, Ross Ice shelf coast, Weddell Ice shelf coast and King Haakon VII sea coast.

ACPD
13, 6807–6849, 2013

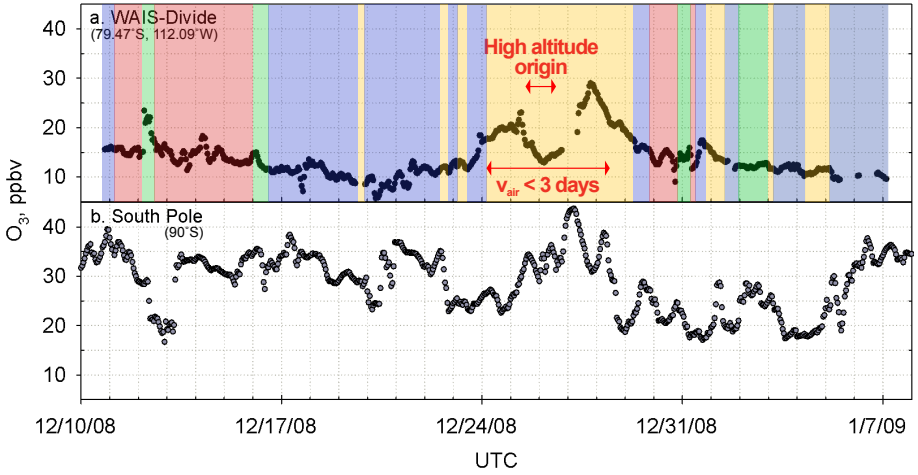

Fig. 9. Ozone observed at WAIS Divide and at South Pole (data available at: http://ds.data.jma.go.jp/gmd/wdcgg) for austral summer 2008–2009. Air-mass origins are reported with the identical color coding used in Fig. 8: East Antarctic Plateau (yellow), regions below East Antarctic Plateau (blue), WAIS (red) and Antarctic coast (green). Events of air transport less than 3 days between East Antarctic Plateau and WAIS Divide and of high-altitude air origin (< 2 km a.g.l.) are also reported.

ACPD
13, 6807–6849, 2013